Journal of Thermal Analysis and Calorimetry, Vol. 61 (2000) 861–871

THERMAL AND SPECTROSCOPIC STUDIES ON THE DECOMPOSITION OF SOME AMINOGUANIDINE NITRATES

S. R. Naidu[1], *K. V. Prabhakaran*[2], *N. M. Bhide*[1] *and E. M. Kurian*[1]

[1]High Energy Materials Research Laboratory, Sutarwadi, Pune
[2]Armament Research and Development Establishment Pune 411021, India

(Received August 4, 1999)

Abstract

Diaminoguanidine nitrate (DAGN) and triaminoguanidine nitrate (TAGN), potential energetic materials in emerging propulsion technology with high mass impetus at low isochoric flame temperature have been studied as regards kinetics and mechanism of thermal decomposition using thermogravimetry (TG), differential thermal analysis (DTA), infrared spectroscopy (IR) and hot stage microscopy. Kinetics of thermolysis has been followed by isothermal TG and IR. For the initial stage of thermolysis of DAGN the best linearity with a correlation coefficient of 0.9976 was obtained for the Avrami-Erofe'ev equation, n=2, by isothermal TG. The activation energy was found to be 130 kJ mol^{-1} and log$A$=11.4. The initial stage of thermolysis of TAGN also obeyed the Avrami-Erofe'ev equation, n=2, with a correlation coefficient of 0.9975 by isothermal TG and the kinetic parameters are E=160.0 kJ mol^{-1} and log$A$=16.0. High temperature IR spectra showed exquisite preferential loss in intensity of the NH_2, NH, N–N stretching and CNN bending. Spectroscopic and other results favour deamination reaction involving the rupture of the N–N bond as the primary step in the thermal decomposition.

Keywords: DAGN, kinetics, mechanism and IR spectroscopy, TAGN, thermal decomposition

Introduction

Energetic materials containing the guanidine functionality can make significant contributions in areas of the emerging propulsion technologies because of their insensitivity and low flame temperature. DAGN and TAGN, members of this guanidine class of energetic amine nitrates have gained special attention because of their manifold unique properties such as capacity to produce relatively low molecular weight gaseous decomposition species. These properties of TAGN are advantageous for realizing higher mass impetus at lower isochoric flame temperature [1–4] due to its molecular structure which contains HNO_3 as the oxidiser part with an extremely high percentage of energetically combined nitrogen in comparison to many energetic materials of current use. There have been a few experimental attempts to study the thermal stability [5–10], structural parameters [11–14], total energy, core–core repulsion energy, charge distribution, heat of formation,

1418–2874/2000/ $ 5.00

Akadémiai Kiadó, Budapest
Kluwer Academic Publishers, Dordrecht

ionization potential, dipole moments of cation, effect of rotation across N–N bonds and the energy barrier for the rotation of the primary amino group, combustion [4] and IR spectra [8, 15–17]. For the effective use of TAGN and DAGN as propellant ingredient a knowledge of the kinetics and mechanism of their thermal decomposition is essential. The present study has been undertaken with this aim using thermal analysis, IR, evolved gas analysis and hot stage microscopy.

Experimental

DAGN [18] was synthesized by reducing nitroamino guanidine with zinc dust and acetic acid below –10°C. TAGN was synthesized by the reported method [19] from guanidine nitrate and hydrazine hydrate. The crude DAGN and TAGN obtained were purified by recrystallisation from water. The particle size of 14 μ was achieved by wet grinding in a colloidal mill. The purity of the sample was confirmed by elemental analysis, melting point, high pressure liquid chromatography and IR. Further experimental details are given in our previous communications [20–25].

Results

Thermal decomposition of DAGN

A number of TG/DTA/EGA curves have been recorded under various conditions and representative ones are presented in Fig. 1. The TG curve of DAGN at a heating rate

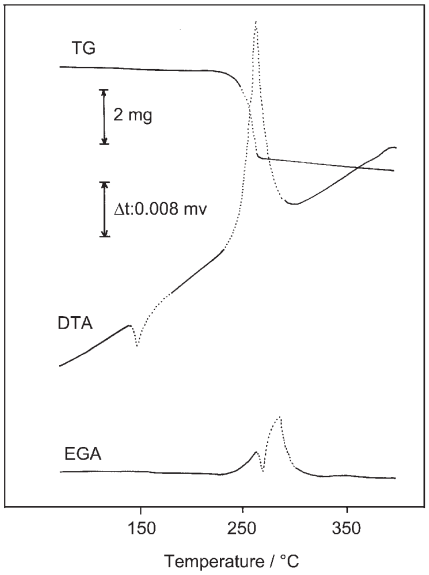

Fig. 1 TG/DTA/EGA of DAGN; sample mass: 10 mg; reference: calcined alumina, atmosphere: dynamic nitrogen (10 l h^{-1})

of 10°C min^{-1} in static air and nitrogen atmosphere indicates a steady curve upto about 236°C and there after a sharp loss in mass of about 35% of the original mass in the range of 236–285°C is observed. This was followed by a fast further mass loss in the range, 285–295°C, which amounts to about 45% of the original mass. The solid residue left behind is about 20% of the original mass.

DTA of DAGN [6] displayed highly exothermic overlapping changes in the range, 236–314°C. DTA also shows an endothermic tendency at 143°C which corresponds to the melting of DAGN. DTA peaks were better resolved at lower heating rates and in fact consists of three distinct stages. EGA curve of DAGN indicates apparently two gas evolution peaks in the range 285–314°C.

Kinetics by isothermal TG

Isothermal TG curve obtained for the thermal decomposition of DAGN at 240°C is given in Fig. 2. It consists of three stages the initial one upto 35% conversion, the second from 35–65% and the third from 65–80% of the original mass and there is definite increase in velocity of the reaction with successive stages. From the isothermal TG data the fraction α that decomposed at any given time t was evaluated. The resultant α–t curves for the initial stage upto 35% at different temperatures are given in Fig. 3. α–t curves were analysed using various kinetic model functions $F(\alpha)$ [20]. The kinetic models which gave better correlation coefficient are given in Table 1 along with the rate parameters obtained. The best linearity was obtained for the Avrami-Erofe'ev equation, n=2, which also gave the best Arrhenius plot with an activation energy of 130 kJ $mol^{-1}$and log$A$=11.4 for the first stage. α–t curves obtained for the second stage, 35–65% α, are given in Fig. 4. The kinetic models which gave better correlation coefficient are given in Table 2 along with the rate parameters obtained. Activation energy of 127 kJ mol^{-1} and log$A$=10 have been assigned to this stage based on the contracting volume equation, $[1–(1–\alpha)^{1/3}]$, which gave the best correlation coefficient and Arrhenius plot.

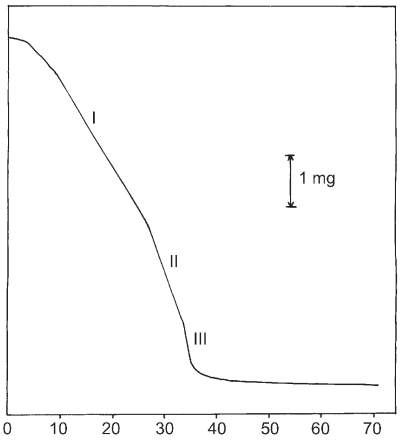

Fig 2 Isothermal TG curve of DAGN at 240°C

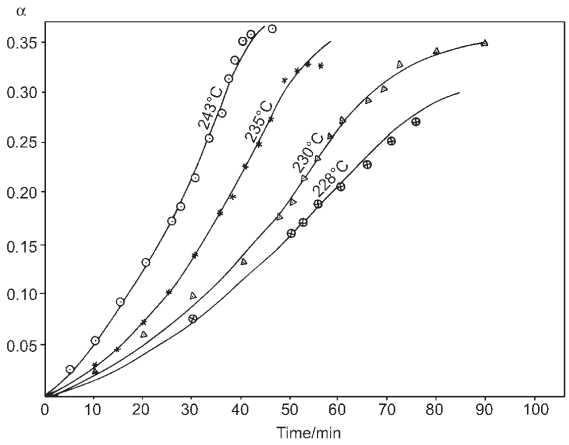

Fig. 3 α–*t* plot for the first stage isothermal decomposition of DAGN (TG)

Table 1 Correlation coefficient *R* obtained for various $F(\alpha)$ and rate parameters by isothermal TG for the first stage decomposition of DAGN

	$F(\alpha)$	*R* at temperature/°C				*E*/ kJ mol^{-1}	log*A*/ s^{-1}
		228	230	235	243		
1	$[1-(1-\alpha)^{1/2}]$	0.9956	0.9677	0.9744	0.9777	125.0	10.0
2	$[1-(1-\alpha)^{1/3}]$	0.9952	0.9647	0.9724	0.9751	125.0	10.0
3	$[-\log(1-\alpha)]$	0.9942	0.9582	0.9681	0.9693	126.0	10.8
4	$[-\log(1-\alpha)]^{1/2}$	0.9964	0.9971	0.9984	0.9985	130.0	11.4
5	$[-\log(1-\alpha)]^{1/3}$	0.9935	0.9941	0.9984	0.9934	134.0	11.7

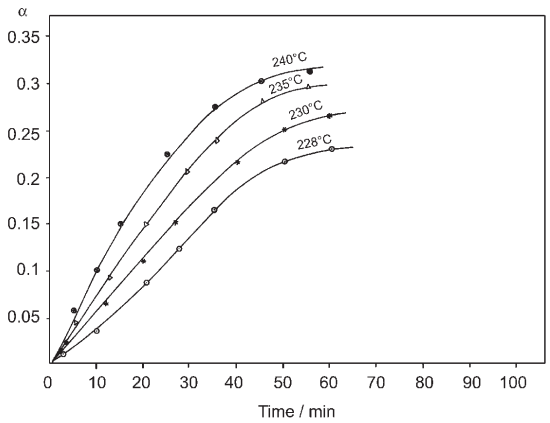

Fig. 4 α–*t* plot for the second stage isothermal decomposition of DAGN (TG)

Table 2 Correlation coefficient R obtained for various $F(\alpha)$ and rate parameters by isothermal TG for the second stage decomposition of DAGN

	$F(\alpha)$	R at temperature/°C				E/ kJ mol^{-1}	log$A$/ s^{-1}
		228	231	235	240		
1	$[1-(1-\alpha)^{1/2}]$	0.9933	0.9938	0.9997	0.9976	125.0	10.0
2	$[1-(1-\alpha)^{1/3}]$	0.9932	0.9946	0.9997	0.9974	127.0	10.0
3	$[-\log(1-\alpha)]$	0.9929	0.9959	0.9995	0.9966	130.0	11.3
4	$[-\log(1-\alpha)]^{1/2}$	0.9735	0.9735	0.9931	0.9923	82.0	6.4
5	$[-\log(1-\alpha)]^{1/3}$	0.9511	0.9609	0.9984	0.9869	63.0	4.4

Evolved gas analysis by IR

Gaseous products of the thermal decomposition of DAGN were analysed using a specially fabricated IR gas cell [18]. Prominent absorption bands observed and their assignments are given in Fig. 5. Ammonia [25] as expected was the initial gaseous product followed by other gaseous products and the variation of gas phase composition with increase in temperature is significant and suggestive of the stagewise decomposition as observed in simultaneous thermal analysis.

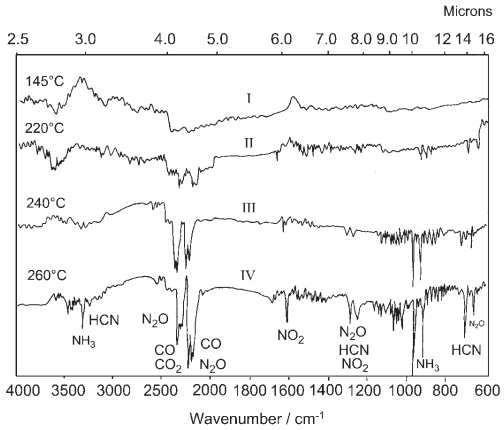

Fig. 5 IR spectra of gaseous decomposition products of DAGN

Effect of additives

α–t plots for DAGN and DAGN mixed with 10% additives such as akardite-1, 2-nitro diphenylamine (2-NDPA), carbamite and diphenylamine (DPA) at 227°C are given in Fig. 6. These indicate that akardite-1 and 2-NDPA accelerated the overall thermal decomposition of DAGN while carbamite accelerated the thermal decomposition reaction upto about 35% of α and then retarded. DPA had an overall decelerating effect on the decomposition of DAGN.

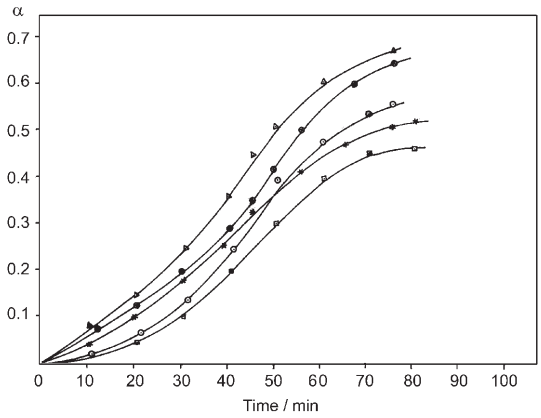

Fig. 6 α–*t* plot for the effect of additives on the isothermal decomposition of DAGN (TG) at 227°C; DAGN; DAGN:CARB; DAGN:2-NDPA; DAGN:AKARDITE; DAGN:DPA

Morphological studies

Photomicrographs obtained during the thermal decomposition of DAGN as a function of temperature under programmed heating rate of 10°C min^{-1} were recorded. They indicate that crystalline DAGN undergoes rapid crystal movements, melting, gradual evolution of gases through localised pipe holes in the melt phase. A black charred residue is left behind in the end.

Thermal decomposition of TAGN

A large number of TG/DTA/EGA of TAGN (Fig. 7) were recorded under different conditions. These do reveal some interesting finer features. The TG of TAGN (Fig. 7) in nitrogen atmosphere at a heating rate of 5°C min^{-1} indicates a steady curve up to about 216°C. Then a sharp change to the extent of about 29 % of the original mass is observed in the range of 216–238°C followed by further mass losses in the range of 238–252°C amounting to about 59% of the original mass. The solid residue left behind is about 12% of the original mass. The results obtained were similar in static air atmosphere.

The DTA of TAGN (Fig. 7) shows overlapping exothermic changes with peak maxima at 224, 245 and 265°C. These consecutive exothermal changes observed in the DTA of TAGN are in agreement with Krien [6] but are at variance with the findings of Kubota *et al.* [9] wherein the latter exothermic DTA changes are considered endothermic. At lower heating rates of 2°C min^{-1} decomposition sets in little earlier at 210°C and the shoulder after the first exotherm is conspicuous. The evolved gas analysis curve of TAGN indicates apparently two dominant gas evolution peaks in the range 225–252°C.

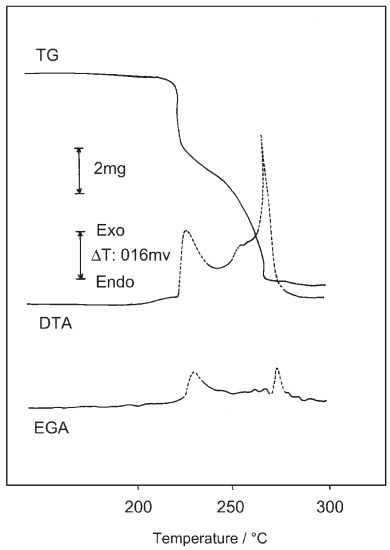

Fig. 7 TG/DTA/EGA of TAGN; sample mass: 10.0 mg, reference: calcined alumina, atmosphere: dynamic nitrogen (10 l h^{-1})

Effect of additives

The effect of metal oxides/additives at 5% level such as nickel oxide, monobasic lead stearate, cupric oxide, copper chromite, lanthanum oxide, titanium dioxide, zirco-

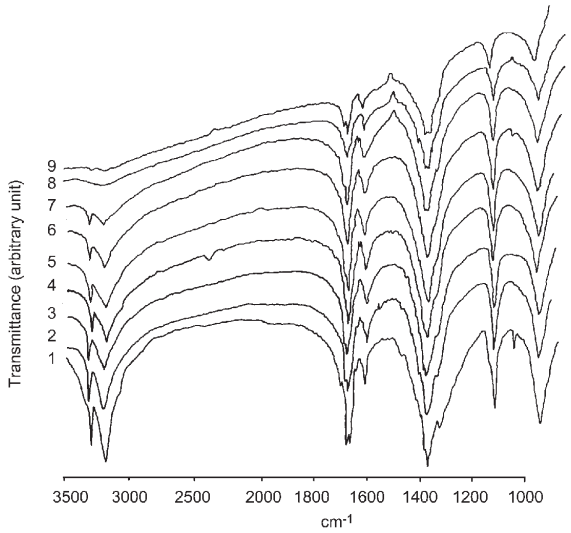

Fig. 8 Time dependence of the IR spectrum of TAGN at 174°C; spectrum – 1 at room temperature and spectra – 2, 3, 4, 5, 6, 7, 8 and 9 are after 0, 60, 90, 120, 150, 180, 210 and 240 min, respectively at 174°C

nium dioxide, cobaltic oxide, cerium oxide, ferric oxide on the DTA exotherm corresponding to the initial thermolysis of TAGN was studied and from these curves, T_i, T_m and T_f were evaluated. It is observed that none of the additives accelerated nor decelerated the initial thermolysis of TAGN.

Kinetics by isothermal TG

The kinetics [20–25] of the thermal decomposition of TAGN at different temperatures under static air was studied by isothermal TG. A representative α–t plot obtained at 210°C is given in Fig. 8. The α–t curve is sigmoidal in nature. The first sigmoidal curve is up to 29% conversion of original mass as in TG. For the first stage at lower temperatures there was close competition between deceleratory, Prout-Tompkin and the Avrami-Erofe'ev equation n=2 and 3 (Table 3). The best linearity was obtained for the Avrami-Erofe'ev equation n=2, $[-\ln(1-\alpha)]^{1/2}$ for the range 0–29% of α which also gave the best Arrhenius plot. The slope of the Arrhenius plot gave an activation energy of 160 kJ mol^{-1} and the intercept log$A$=16.0.

Table 3 Correlation coefficient R obtained for various $F(\alpha)$ and rate parameters by isothermal TG for the first stage decomposition of TAGN

	$F(\alpha)$	R at temperature/°C				E/ kJ mol^{-1}	log$A$/ s^{-1}
		173	179	184	190		
1	$\alpha^{1/3}$	0.9983	0.9880	0.9937	0.9197	156.0	15.6
2	$[-\log(1-\alpha)]^{1/2}$	0.9973	0.9953	0.9995	0.9879	160.0	16.0
3	$[-\log(1-\alpha)]^{1/3}$	0.9984	0.9912	0.9973	0.9783	155.0	15.0
4	$[-\log(1-\alpha)]^{1/4}$	0.9983	0.9884	0.9947	0.9723	152.0	15.0
5	$[\log\alpha/(1-\alpha)]$	0.9967	0.9804	0.9863	0.9563	147.0	15.0

High temperature IR spectroscopy

IR spectra of TAGN in KBr matrix was recorded at elevated temperatures as a function of time and spectra obtained at 174°C are reproduced in Fig. 8. Sharp preferential loss in absorbance of NH_2 band at 3317 and 3214 cm^{-1} (γ_{as} NH) is significant to that of NO_3 at 1385 and 1335 cm^{-1}. Similar results have been obtained for DAGN too. Preferential loss in related bands like N–N stretch at 1129 cm^{-1} and CNN bend at 955 cm^{-1} to that of NO_3 is also discernible [8, 9, 26–27]. The band at 1129 cm^{-1} has been assigned to N–N stretch [8] as well as C–N stretch [9]. In the IR spectrum of guanidine nitrate which has C–N bond but no N–N bond the band at 1129 cm^{-1} is prominent [9]. Our IR spectrum of TAGN at room temperature reveals that the band around 1129 cm^{-1} has a shoulder (Fig. 8 spectrum 1). The band at 1129 cm^{-1} is partially retained even after the complete loss in intensity of the amino band when no N–N band remained (Fig. 8 spectrum 9). We are therefore of the opinion that the band around 1129 cm^{-1} has to be attributed to both N–N and C–N stretching frequencies overlapping.

Discussion

TAGN in the crystalline state has orthorhombic Pbcm space group [11–12] with infinite three dimensional network of N–H–O–H bonds linking the triaminoguanidium ion to the NO_3 ion. The C–N bonds are considered equivalent and the mean C–N distance is 1.331 Å and is indicative of a partial double bond which is consistent with a model having recourse to three equivalent structures. The N–N bond length shows some variation and the mean 1.403 is much shorter than 1.45 Å reported for TAGCI showing that there is negligible double bond character between N–N atoms vide Scheme 1:

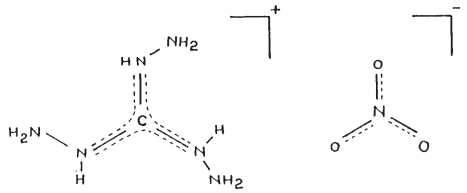

Scheme 1

Simultaneous TG, DTA and EGA results indicate that the thermal decomposition of TAGN occurs stagewise and three initial stages are exothermic. The molecular weight fraction of the three amino groups within the TAGN molecule is 0.29 and the formation of three ammonia molecules constitute a loss of 0.30 mass fraction. The observed mass loss fraction in the TG first stage is about 0.29. This is suggestive of the deamination reaction within the TAGN molecule in the first stage through the clevage of the N–N bond leading to the formation of the NH_2 radicals which consecutively abstract hydrogen atoms from the parent molecule giving rise to ammonia.

IR spectra of TAGN recorded during the course of decomposition (Fig. 8) show that the amino group and related absorption bands disappear first before the rest of the absorption band intensities get affected. The intermediate product after the loss of the amino group intensities retains all the rest of the absorption bands of the parent molecule with the intensities practically intact in our studies [26–27] using KBr pellet method as also observed by Brill *et al.* [8] elegantly in their studies on the temperature dependence of the IR spectra of polycrystalline TAGN suspended between two NaCI plates at a heating rate of 5°C min^{-1}. The IR spectra obtained after the loss of the amino and related band intensities and the one obtained after the first stage decomposition in TG are similar (Fig. 8 spectrum 9). These results suggest the cleavage of the N–N bond initially [24–25]. When N–N bond rupture occurs homolytically the formation of NH_2 free radical is corollary and this free radical can abstract a hydrogen atom from the TAGN molecule to form ammonia and give rise to another free radical derived from the parent molecule, leading to a radical induced chain reaction. This conclusion is also consistent with the findings based on the studies of the alkyl ammonium salts [28] in which when a second type of energetic functional group is present in the cation, the energetic site that triggers the decomposition reaction is this en-

ergetically substituted cationic group, when the latter is more thermally labile, rather than the de-neutralisation reaction at $NH_3^+NO_3^-$ site leading to $HNO_3(g)$.

It may be noted that the bond dissociation energy of the N–N bond is of the order of 160.5 kJ mol^{-1} [9, 29] and the activation energy obtained for the first stage decomposition by isothermal TG is also about 160.0 kJ mol^{-1} showing thereby that the rate controlling step in the first stage thermolysis of TAGN involves N–N bond fission in conformity with the esquisite preferential intensity loss of the NH_2, N–N and CNN bend in IR. Detection of ammonia as the primary gaseous product in EGA by IR and GC-MS studies [4] and the results obtained by Kubota *et al.* [9], that the energy released through the rupture of the N–N bond is the heat produced at the early stage of decomposition and the HNO_3 attached to the molecular structure of TAGN is not the fragment responsible for the rapid exothermic reaction observed at the early stages of the thermal decomposition process also corroborate N–N bond fission as the primary step. The second stage may involve the formation of NO_2 radical and subsequent oxidative degradation leading to stable products. The formation of thermally stable polymerised solid residue in the end also supports the involvement of free radicals in the thermal decomposition.

DAGN crystal structure [14] belongs to the space group P1. In DAGN cation, $[(NH_2NH)_2C(=NH_2)^+]$, the carbon and the nitrogen atoms are coplanar. Crystal shows N–N bond paths rather than N–H bond paths expected for true hydrogen bonded structures; and only five of the hydrogens out of the eight are involved in N–H···O hydrogen bonds. In DAGN the conformation with an *S* configuration for DAGN cation is favoured energetically where one of the terminal NH_2 groups is *cis* to the central $C{=}NH_2$ bond and the other is *trans* as shown in Scheme 2:

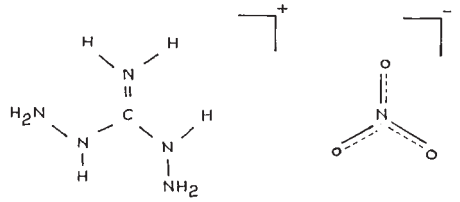

Scheme 2

These structural characteristics [24] indicate that in DAGN too, as in TAGN, deamination reaction is favoured primarily in the thermolysis. This is confirmed by high temperature IR studies of DAGN wherein the spectra obtained as a function of time is similar to those of TAGN vide Fig. 8, wherein the preferential loss in intensity of the amino and related bands are uniquely distinct. The formation of ammonia as the gaseous product in the initial stages [27] as in TAGN also substantiates the deamination reaction in the first stage.

The activation energy obtained is also consistent with the expected N–N bond dissociation energy. As the reaction proceeds the rupture of the $O–NO_2$ bond occurs in the second stage (Fig. 3) resulting in the generation of reactive NO_2 radical leading to further acceleration in the rate of decomposition. This is indicated by the promi-

nent loss in intensity of the nitrate band in the spectrum recorded during this stage. Rapid increase in the decomposition rate experimentally observed after 65% may be attributed to the branching of the chain in the radical induced chain reaction operative. An analogous mechanism for TAGN and DAGN decompositions are thus mutually corroborative.

References

1 V. E. Huary and M.B. Frankel, US. Patent 3732131, 8 May 1973.
2 Rock Well Int. Fr. Damande, 730073, 5 Jan. 1973.
3 V. B. Haury, J. E. Flanagan and M. B. Frankel, Rockwell Int. Copn. Ger. Offen 2263860, 28 Dec. 1972.
4 E. Flanagan, JANNAF, Combustion Meeting, CPIA Publication 6l.,Vol 1, De.c 1974, 285.
5 Y. P. Chrignan and D. R. Satriana, J. Org. Chem., 32 (1967) 285.
6 G. Krien, Explosiv Stoffe, 13 (1965) 211.
7 Y. Oyumi, A. L. Rheingold and T. B. Brill, Propellants, Explos. Pyrotech., 12 (1987) 46.
8 Y. Oyumi and T. B. Brill, J. Phys.. Chem., 89 (1985) 4325.
9 N. Kubota, N. Hirata and S. Sakamote, Propellants, Explos. Pyrotech., 13. (1988) 65.
10 C. F. Melius, 'Chemistry and Physics of Energetic Materials', S. N. Bulusu (ed.), Kluwer Boston, 1990.
11 V. S. Choi and E. Prince, Acta Crystallogr., Sect. B, 35 (1979) 760.
12 A. J. Bracuti, Acta Crystallogr., Sect.B, 35 (1979) 761.
13 P. D. Martinez, Propellants, Explos. Pyrotech., 18 (1993) 83.
14 J. P. Ritchie, K. Y. Lee, D. T. Cromer, E. M. Kober and D. D. Lee, J. Org. Chem., 55 (1990) 1994.
15 E. Liber, D. R Levering and L. J. Patterson, Anal. Chem., 23 (1951) 1594.
16 W. D. Kumler, J. Amer. Chem. Soc., 43 (1965) 1154.
17 M. Trembly, Can. J. Chem., 43 (1965) 1154.
18 J. F. Thorpe and M. A. Whitely, Thorpe's Dictionary of Applied Chemistry IV. Ed. Longmans Green and Co. New York, 6 (1943) 148.
19 J. P. Picard, Morristown Danie, R. Satriana Verona and Frank J. Masuelli, US patent 3813439 Patented May 28, 1974.
20 K. V. Prabhakaran, N. M. Bhide and E.M.Kurian, Thermochim. Acta, 220 (1993) 169.
21 K. V. Prabhakaran, N. M. Bhide and E. M. Kurian, Thermochim. Acta, 241 (1994) 199.
22 K. V. Prabhakaran, S. R. Naidu and E. M. Kurian, Propellants, Explos., Pyrotech., 20 (1995) 238.
23 K. V. Prabhakaran, N. M. Bhide and E. M. Kurian, Thermochim. Acta, 249 (1995) 249.
24 P. S. Makashir and E. M. Kurian, J. Thermal Anal., 46 (1996) 225.
25 S. R. Naidu, K. V. Prabhakaran, N. M. Bhide and E. M. Kurian, J. Thermal Anal., 44 (1995) 1449.
26 K. V. Prabhakaran, Studies on the Reactivity of Triamino, M. Sc. Thesis, University of Pune, 1984.
27 R. Naidu, Studies on the Solid State Reactivity of Some Guanidine Compounds, M. Sc. Thesis, University of Pune, 1986.
28 Y. Oyumi and T. B. Brill, J. Phys. Chem., 91 (1987) 3657.
29 L. Pauling, 'The Chemical Bond' Oxford University Press, London 1967, p. 601.